Opto-Electronics Review

journal homepage: https://journals.pan.pl/opelre

Intelligent transportation: a hybrid FSO/VLC-assisted relay system

Suzan M. EL-Garhy[a,b*], Ashraf A. M. Khalaf[b], Moustafa H. Aly[c], Mohamed Abaza[c]

[a] Electronics and Communications Department, College of Engineering, Higher Technological Institute, Tenth of Ramadan, Egypt
[b] Electronics and Communications Department, Faculty of Engineering, Minia University, Egypt
[c] Electronics and Communications Department, College of Engineering and Technology, Arab Academy for Science Technology and Maritime Transport, Egypt

Article info

Article history:
Received 24 Sep. 2022
Received in revised form 14 Nov. 2022
Accepted 28 Nov 2022
Available on-line 29 Dec. 2022

Keywords:
Intelligent transportation systems; infrastructure-to-vehicle; vehicle-to-vehicle; relay.

Abstract

Various intelligent transportation systems are proposed in different forms of wireless communication technologies. Recently, the importance of visible light communication and free-space optics has been demonstrated in accomplishing vehicle-to-vehicle and infrastructure-to-vehicle communication systems, due to power efficiency, free licenses, and safety for human health. In this paper, a new hybrid relay system supported by free-space optics/visible light communication with two scenarios is proposed. The first one is that the data are transferred from the source to the relay through a free-space optics communication link and are then directed to the destination through a visible light communication link. The second scenario is that the data are transmitted from the source to the destination passing through two different relays to ensure larger coverage. A 10^{-6} bit error rate is achieved at a distance of 900 m for the first scenario with a remarkable signal-to-noise ratio of ~25.5 dB, while the largest distance that can be covered by the second scenario is 1200 m with a signal-to-noise ratio of ~30 dB.

1. Introduction

The intelligent transportation system (ITS) is a technology that offers traffic management as it provides safe travel for both roads and humans [1]. ITS is now one of the most indispensable solutions that provide communication and information technologies to maintain a solution to the traffic congestion, as well as other traffic control issues. Moreover, to ensure efficient traffic and software exchange, it is also essential to combine data transfer, real-time monitoring, and data mining technologies [2]. Since it is more affordable and does not require 'licencing' or new infrastructure, the optical wireless communication (OWC) technology is recommended in ITS as a whole of other optical wireless systems [3]. It is well known that road accidents overtook other causes of death in 2020 [4, 5]. Day by day, the road traffic volume increases and thus, the number of traffic accidents increases. To overcome this problem, which makes the public unsafe, advanced technologies are required. Technologies have been created to monitor and manage vehicles, reducing traffic congestion, delay, and accidents [3].

The term OWC denotes the transmission of information using optical signals over wireless media. OWC has advantages over radio frequency (RF) technology, such as fast data transmission, license-free spectrum, secure data transmission, affordable installation, etc. Additionally, it includes short-range communication between integrated circuit connections, as well as indoor, outdoor, satellite, and terrestrial communication [2]. A new technique called visible light communication (VLC) transmits and receives data using existing LEDs and photodetectors [6], respectively [7]. On the other hand, free-space optics (FSO) communication links can be used for both academic and commercial purposes because they are easy to establish and offer secure connection. FSO uses an infrared band with a

*Corresponding author at: suzan.mohammed@hti.edu.eg

https://doi.org/10.24425/opelre.2022.144260
1896-3757/ Association of Polish Electrical Engineers (SEP) and Polish Academic of Sciences (PAS). Published by PAS

high-capacity bandwidth, making it suitable for outdoor links [8]. Currently, it provides many services, including outdoor wireless access, storage area networks (SANs), last-mile access, enterprise connection, fibre backup, etc. [8, 9]. The effectiveness of FSO is influenced by several external parameters, including atmospheric turbulence, path loss, and pointing errors. Multiple channel models, including log-normal (L-N), gamma-gamma, and double-generalised gamma (DGG), Malaga, etc., are used to simulate the effects of air turbulence [10].

Most VLC systems rely on a line-of-sight (LOS) transmission. Admittedly, LOS is not always promising, especially when dealing with the outdoor environment due to the surrounding interference from the ambient light and the limited coverage. Furthermore, various weather conditions, like rain and fog, are considered as drawbacks of the VLC channel. On the other hand, as the VLC systems enable positioning applications (such as transmitting lane identifier from the LED traffic light to a vehicle), and are bio-secure and license-free, it makes them preferable to RF systems. Consequently, the concept of hybrid systems was established. In Ref. 11, the disadvantages of RF and the limitations of VLC system were overcome by offering the advantages of both systems that ensure a long-distance transmission, but on the other hand, the risk factor of RF system was considered. Rima *et al*. [6] introduced the performance of a hybrid VLC-FSO-VLC co-operative system with decode-and-forward (DF). For outdoor applications [12], a system model was suggested for combining FSO and RF channels under various weather conditions. In contrast, Momen *et al*. [13] proposed a VLC/RF co-operative system and compared its performance with a stand-alone VLC system.

In this paper, a new hybrid FSO/VLC-assisted relay system with an image sensor receiver, instead of a single photodiode, is proposed in two different scenarios. The first hop links the source (S) and the relay (R) through the FSO communication channel. The relay (R) and the destination (D) are connected through a VLC link. In this FSO/VLC system, R-D VLC links contain LED luminaries under the assumption that the emitted light from the LED is characterised by a Lambertian radiation pattern. The FSO link between S-R is characterised by pointing errors, path loss, and L-N weak turbulence channel at which total energy is minimized while maintaining a reliable communication system. A study of performance of signal-to-noise ratio (SNR) and bit error rate (BER) at different coverage distances was performed. Furthermore, multi-hops of relay scenarios were applied to achieve a wider coverage area with an acceptable BER.

This paper is arranged as follows. The structure and design of the proposed system is presented in section 2. The mathematical model is introduced in section 3. Section 4 represents the obtained results and discussion. Section 5 is showing the main conclusions.

2. System structure and design

A real scenario for the FSO/VLC-assisted relay system is explained in Fig. 1. Using a relay achieves a longer coverage area. Vehicle number 1 can receive the traffic information such as crowded area or traffic accident from the light traffic through the FSO link passing through relay 1 at a distance up to 500 m from relay 1 and 500 m from the traffic light to relay 1 with an acceptable BER. Vehicle number 2, which is far away from the traffic light by a distance longer than 1 km, can receive the traffic data from the relay mounted in vehicle number 1 through the VLC link. In other words, the first hop supports an FSO link connecting the source (S) to relay 1 (R_1). The second hop R_1 and relay 2 (R_2) are connected via the FSO link. Furthermore, the third hop connects R_2 and the destination (D) via the VLC link.

In the VLC link, the optical signal is intensity-modulated (IM). ψ is the incident angle and φ denotes the irradiance angle. The half power semi-angle of the LED traffic light $\Phi_{1/2}$ is 15°. The traffic light height is H_1 = 5.3 m, the height of the receiver denotes H_r = 1 m, and the location of the vehicle can be represented by the distance in direction of the lane x and the distance in the lane width direction y, as shown in Fig. 1(b).

At the receiver, it seems that the signal is detected and processed at once, and the resulting signal can have unwanted signals, background noise, etc. As a result, the system performance will suffer from the undesired signals. An alternative to the avalanche photodiode (APD) is a 2-dimensional (2D) image sensor to be able to reduce the device complexity and the impact of unwanted signals [13]. Each pixel will have an independent field of view (FoV) when used as a receiver in a 2D image sensor. As a result, most unwanted messages can be diminished.

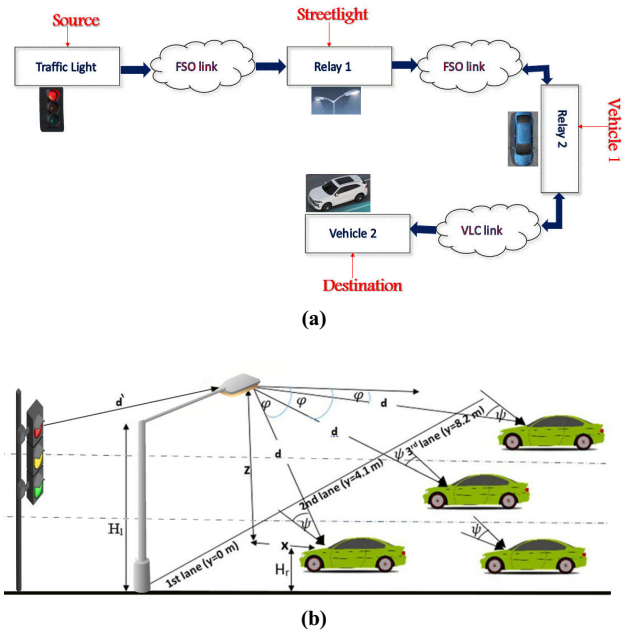

Fig. 1. The block diagram presents the FSO/VLC hybrid system (a) and the proposed system model for the FSO/VLC hybrid system (b).

3. Mathematical model

3.1. FSO mathematical model

The normalized channel coefficient of the FSO system is calculated by [14]

$$h = h_a h_\beta h_p, \tag{1}$$

where h_a represents the atmospheric turbulence coefficient of channel fading, h_p refers to the channel coefficient resulting from a misalignment error, and h_β denotes the path loss that can be obtained by [14]

$$h_\beta = 10^{-\alpha d'/10} \times \frac{D_R^2}{(D_T + \theta_T d')^2}, \tag{2}$$

where the distance between source and relay is denoted by d', α refers to the coefficient of the dependent attenuation of weather, D_T is the transmitter aperture diameter, D_R is the receiver aperture diameter, and θ_T is the divergent angle of the optical beam.

The channel fading coefficient due to the misalignment error is obtained by [15]

$$h_p \approx A_0 \exp\left(\frac{-2r^2}{w_{zeq}^2}\right), \tag{3}$$

where r is the radial displacement, which is modelled by the Rayleigh distribution knowing that the corresponding beam width is given by [15]

$$w_{zeq}^2 = \frac{w_z^2\sqrt{\pi}\,\mathrm{erf}(\upsilon)}{2\upsilon \exp(-\upsilon^2)}, \tag{4}$$

where w_z is the beam waist and

$$\upsilon = \frac{\sqrt{\pi} D_R}{2\sqrt{2} w_z}. \tag{5}$$

Notice that A_0 is the collected power fraction at $r = 0$ and is measured by the error function, $\mathrm{erf}(\cdot)$ in [16] as

$$A_0 = [\mathrm{erf}(\upsilon)]^2. \tag{6}$$

The radial displacement $f_r(r)$ is modelled as in [15]:

$$f_r(r) = \frac{r}{\sigma_s^2}\exp\left(-\frac{r}{2\sigma_s^2}\right), \quad r > 0, \tag{7}$$

where ${\sigma_s}^2$ is the receiver jitter variance.

3.1.1. L-N channel model

The L-N channel probability density function (PDF) is given by [15]

$$f_h = \frac{\xi^2 h^{(\xi^2-1)}}{2(A_0\beta)^{\xi^2}}\mathrm{erfc}\left(\frac{\ln\left(\frac{h}{A_0\beta}\right) + q}{\sqrt{8}\sigma_x}\right)\exp\left(2\sigma_x^2\xi^2(1+\ \xi^2)\right)$$

where $\mathrm{erfc}(\cdot)$ indicates the complementary error function [17] and β is the normalized path loss coefficient, modelled as

$$\beta = {h_\beta}/{\beta_h}, \tag{9}$$

where β_h is the first hop path loss.

The variance is

$$\sigma_x^2 = 0.30545 k^{7/6} C_n^2 d'^{11/6}, \tag{10}$$

where the refractive index parameter is designated as C_n^2, $k = (2\pi/\lambda)$ is the wave number, λ refers to the wavelength of the transmitted signal, and σ_x^2 is the variance of the independent and identically distributed Gaussian random variables in (8).

$$q = 2\sigma_x^2(1 + 2\xi^2), \tag{11}$$

and ξ is the ratio between the receiver equivalent beam width and the standard deviation of the receiver pointing error displacement, given by [18]

$$\xi = \frac{w_{zeq}^2}{2\sigma_s^2}. \tag{12}$$

The coefficient of the channel fading h_a is given by [14]:

$$h_a = \exp(2x), \tag{13}$$

where x is the Gaussian random variable (RV) independent and identically distributed with the mean μ_x and the variance σ_x^2. To assure that the average power is not reduced or amplified by the fading channel, the fading coefficients are normalized [18, 19].

3.2. VLC mathematical model

The transmitted power from each LED is [13]

$$P_{tr}(\varphi) = \frac{m+1}{2\pi} P_t \cos^{m+1}(\varphi), \tag{14}$$

where P_t is the average transmitted optical power, φ denotes the irradiance angle, and m is the Lambertian emission order formulated as

$$m = \left[\frac{\ln 2}{\ln\left(\cos\left(\Phi_{1/2}\right)\right)}\right], \tag{15}$$

where $\Phi_{1/2}$ is the half power semi-angle.

The direct current channel gain $h(0)$ in the optical wireless communication channel is given by [13, 20]

$$h(0) = \begin{cases} \left[\frac{(m+1)A'}{2\pi d^2}\right]\cos^m(\varphi) T_f(\psi) T_{c,i}(\psi)\cos(\psi) & 0 \le \psi \le \psi \\ 0 & \psi \ge \psi_c \end{cases}$$

where A' denotes the detector physical area, $T_f(\psi)$ indicates the constant of filter transmission, d is the LOS distance between source and receiver, and $T_{c,i}(\psi)$ is the fraction of the image size on the i^{th} pixel given by [21]

$$T_{c,i}(\psi) = -0.1982\psi^2 + 0.0425\psi + 0.8778, \tag{17}$$

where ψ is the incident angle.

The vehicle location is defined by the distance in the lane direction x', as well as the width direction y, while z is the height difference between the height of the source of light and the height of the receiver in the vehicle. The LOS distance between the source and the receiver can be calculated by [13]:

$$d = \sqrt{x'^2 + y^2 + z^2}. \tag{18}$$

The angle of irradiance is expressed by [13]

$$\varphi = \cos^{-1}\left(\frac{x'}{d}\right). \tag{19}$$

The angle of incidence is defined as [13]

$$\psi = \cos^{-1}\left(\frac{\sin\left(\theta + \tan^{-1}\left(\frac{z}{x'}\right)\sqrt{x'^2 + z^2}\right)}{d}\right), \tag{20}$$

where θ is the vertical inclination of the receiver.

3.2.1. *Receiver model*

The desired pixel power can be obtained by [13]

$$P_{rx,i}(t) = P_{tr}(\varphi)h(0). \tag{21}$$

Thus, the total received signal is [13]

$$P_t(t) = P_{rx,i}(t) + n(t), \tag{22}$$

where $n(t)$ is the noise component.

Thus,

$$P_t(t) = P_{tr}(\varphi)h(0) + n(t). \tag{23}$$

The noise variance at the i^{th} pixel is approximately calculated by [13]

$$\sigma^2 = 2eRI_2\left(P_{b,i} + P_{rx,i}\right)B + \frac{8\pi k_B T}{G}\eta\hat{\text{A}}I_2B^2 + \frac{16\pi^2 k_B T\Gamma}{G_m}\eta^2\hat{\text{A}}I_3B^3, \tag{24}$$

where $P_{b,i}$ indicates the detected ambient light power by the i^{th} pixel and R is the responsivity of the detector, e is the electron charge, I_2 and I_3 are the constants indicating bandwidth factor of the noise, while B represents the bandwidth desired depending on the modulation technique applied and the bit rate used, k_B is the Boltzmann constant, η is the capacitance per unit area, T is the absolute temperature, G is the open-loop voltage gain, Γ indicates the channel noise factor of the FET, G_m is the conductance of the FET, and $\hat{\text{A}}$ is the detector effective area given by

$$\hat{\text{A}} = \begin{cases} A\cos(\varphi), & \varphi < \text{FoV} \\ 0 & \geq \text{FoV} \end{cases}. \tag{25}$$

Regarding (24), the first part represents the shot noise which acts as the predominant noise in a wireless optical communication (WOC). The second part is the thermal noise of the feed-back resistor. The third part is the thermal noise from the channel resistance of the field effect transistor (FET).

When using an image sensor with a lot of tiny pixels, all three parts of the noise equation can be minimized. Because the received ambient light power is reduced due to the small FoV associated with a small pixel size, therefore, the first part is reduced, while the second and third parts are reduced as the preamplifier input capacitance is reduced because the pixel size of the image sensor is very small.

The amount of the detected ambient light by the i^{th} pixel is determined by the FoV of the pixel and can be estimated as [13]

$$P_{b,i} = 4\pi AB_{\text{sky}}\Delta\lambda T_f T_{c,i}\cos(\psi_i)\sin^2\left(\frac{\psi_{a,i}}{2}\right), \tag{26}$$

where B_{sky} refers to the skylight power spectral density, $\Delta\lambda$ is the bandwidth of the filter, and $\psi_{a,i}$ denotes the pixel detector FoV.

The maximum FoV angle ($\psi_{c,max}$) is denoted as [13]

$$\psi_{c,max} = \tan^{-1}\frac{u}{f}. \tag{27}$$

Such that

$$\theta + \psi_{c,max} \leq 90^{\circ}, \tag{28}$$

where u is the distance between the border of the image sensor and its centre and f is the lens focal length.

The output signal is proportional to the input signal and can be formulated as [22]

$$y_i(t) = x_i(t)\otimes Rh_i(t) + n_i(t). \tag{29}$$

where $h_i(t)$ represents the impulse response of the channel, and $n_i(t)$ represents the additive noise, and ⊗ denotes the convolution.

4. Result and discussion

In this section, the error performance is used to evaluate the proposed system. The SNR is investigated while ensuring an acceptable coverage distance. Tables 1 and 2 illustrate the parameters used in VLC and FSO systems, respectively.

Table 1.
Numerical parameters of the VLC system [13].

Parameter	Symbol	Numerical value
Noise bandwidth factor	I_3	0.868
Boltzmann constant	k_B	1.3811×10^{-23} J/K
Noise bandwidth factor for white noise	I_2	0.562
Transmission power	P_t	150.72 mW
Data rate	R_b	1 Mbps
Absolute temperature	T	298 K
Vertical inclination	θ	45°
Detector responsivity	R	0.35 A/W
Focal length	f	10 mm
Light detector area	A'	3.142 cm^2
Receiver FoV	$\psi_{1/2}$	45°
Electric charge	e	1.602×10^{-19} C
PSD of skylight	B_{sky}	43.0 mW/m^{2}sr·nm
Voltage gain	G	10
Bandwidth of filter	$\Delta\lambda$	83.0 nm
FET transconductance	G_m	30 mS
FET channel noise factor	Γ	1.5
Capacitance per unit area	η	112.0 pF/m^2

Table 2.
Numerical parameters used in the FSO system [18].

Parameter	Symbol	Numerical value
Beam waist (weak-to-strong pointing error)	ω_z	2 m
Wavelength	λ	1550 nm
Jitter standard deviation	σ_s	0.3 m
Receiver diameter	D_R	0.2 m
Attenuation coefficient	α	0.43 dB/km
Transmitter diameter	D_T	0.2 m
Divergence angle	θ_T	2 mrad
Distance between source and destination	d	600–1200 m

4.1. SNR vs. distance of FSO/VLC for S-R-D scenario

Figure 2 displays the relation between SNR and distance at BER = 10^{-6} for the S-R-D scenario. It is taken under consideration that the distance in FSO hop varies from 100 m to 500 m, while it is fixed to 500 m for VLC hop. By increasing the distance, the SNR increases to reach the targeted BER. It is shown that at a distance of 100–500 m (~600 m) (i.e., the distance between S and R *via* FSO link is 100 m, and the distance between R and D is 500 m *via* VLC reaching the total distance between S and D equals 600 m) and 400–500 m (~900 m), the SNR increases from ~16.3 dB to ~25.5 dB which is equivalent to increasing SNR by 9.2 dB to increase the coverage distance from 600 m to 900 m with BER = 10^{-6}.

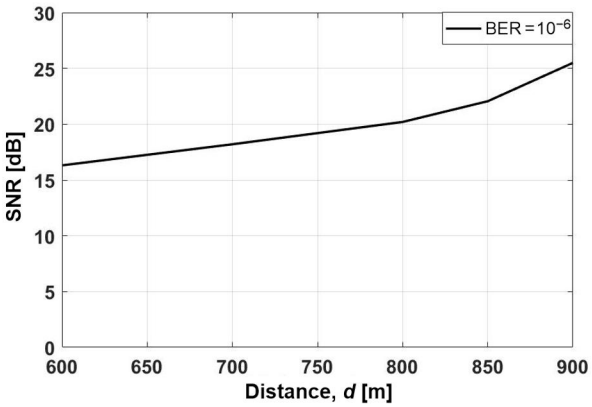

Fig. 2. Relation between distance and SNR for the S-R-D scenario at BER = 10^{-6}.

4.1.1. SNR vs. distance of FSO/VLC system for S-R$_1$-R$_2$-D scenario

The SNR of S-R$_1$-R$_2$-D senario is presented in Fig. 3 at different distances, targeting BER = 10^{-6}. In order to achieve a larger coverage area, two FSO hops and one VLC hop are applied. The distance of the first and the second FSO hop varies from 100 m to 350 m while the third hop of VLC is set at 500 m from R$_2$. It is worth to notice that in order to increase the coverage distance, it is necessary to increase the transmitted power. Moreover, it is shown that by increasing the number of relays from one relay in Fig. 2 to two relays in Fig. 3, the coverage distance increases with acceptable error performance and minimum power consumption. At a distance of 350–350–500 m (1200 m), which is the largest coverage area at BER = 10^{-6}, the SNR is ~30 dB. It is clear that the S-R$_1$-R$_2$-D scenario achieves a larger coverage area than that of S-R-D scenario with an acceptable SNR.

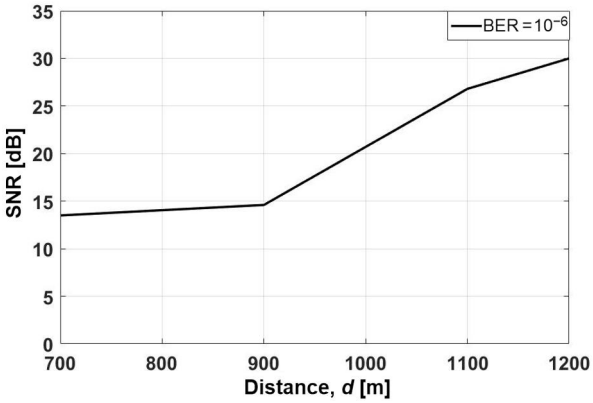

Fig. 3. Relation between distance and SNR at BER = 10^{-6} for the S-R$_1$-R$_2$-D senario.

Comparing the two senarios, it is observed that the S-R$_1$-R$_2$-D gives a better performance of BER, power consumption, and coverage distance than that of S-R-D. At a distance of 900 m and BER = 10^{-6}, both senarios attain 10^{-6}, it is observed that the SNR for S-R-D and S-R$_1$-R$_2$-D scenarios is ~25.5 dB and ~14.5 dB, respectivly.

4.2. Error performance of FSO/VLC system for S-R-D scenario

Figure 4 explains the simulation performed between BER and SNR over the L-N channel for a weak turbulence, with a distance varying from 100 m to 500 m for the FSO hop and 500 m for the VLC hop. One relay is included, and the beam waist is 2 m. It is worth noting that increasing the transmitted power enhances the BER performance. Furthermore, it is clear that the S-R-D at a distance of 100–500 m (600 m) achieves the best performance in terms of power and BER. It also indicates that incrementing d from 100–500 m to 400–500 m leads to increase the SNR from ~16.3 dB to ~25.5 dB at a nominated BER value. Moreover, fixing the d value will improve BER performance by increasing SNR. This shows a fair agreement with the idea of enhancing the BER while improving the transmitted power.

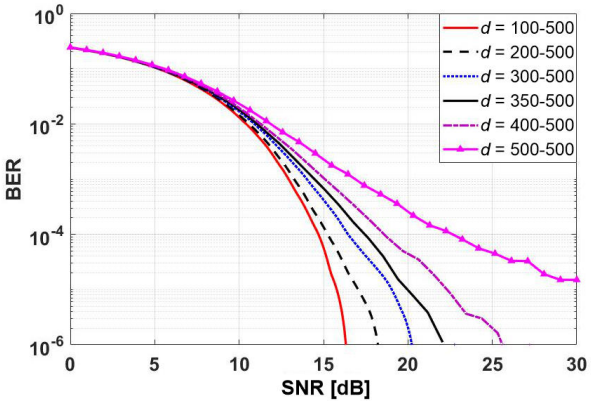

Fig. 4. BER against SNR for a hybrid FSO-VLC system at different distances.

4.2.1. *Error performance of FSO/VLC system for S-R_1-R_2-D scenario*

Figure 5 displays the relation between SNR and BER for the S-R_1-R_2-D senario in order to increase the coverage distance with the targeted BER. It is clear that the BER performance is enhanced by increasing the signal power. Also, increasing the coverage distance will degrade the system performance. It is shown that the distances of 100–100–500 m (700 m) and 200–200–500 m (900 m) achieve BER = 10^{-6} with SNR of ~13.5 dB and ~14.5 dB, respectively. At a distance of 350–350–500 m (= 1.2 km), it also achieves BER = 10^{-6} with SNR = 30 dB.

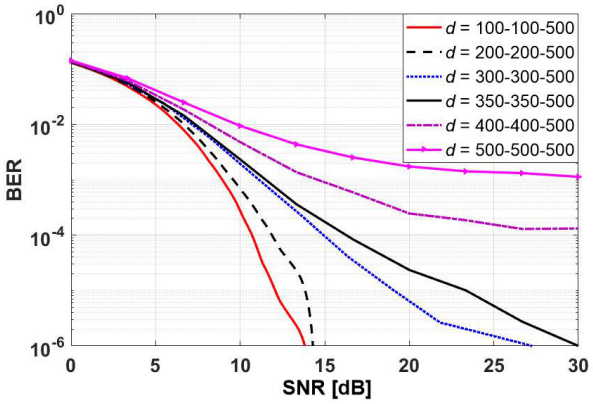

Fig. 5. BER *vs*. SNR for a hybrid FSO/VLC system at different distances for two FSO hops and one VLC hop.

5. Conclusions

A hybrid FSO/VLC-assisted relay system for ITS provides infrastructure-to-vehicle communication via FSO link while establishing vehicle-to-vehicle communication link via VLC using an image sensor as a receiver. The system targets a BER of 10^{-6} and its performance is evaluated by calculating the SNR at different coverage distances. Moreover, in order to increase the coverage distance with a minimum required transmitted power, multi-hops relays are inserted between the source and destination instead of a single relay to attain a reliable communication system. By comparing the first scenario (one relay R_1) with the second scenario (two relays R_1 and R_2), it is noticed that to achieve a coverage distance of 900 m at a targeted BER of 10^{-6}, the SNR for both scenarios is 25.5 dB and 14.5 dB, respectively. Furthermore, it was obtained that increasing the number of hops leads to increasing the coverage distance.

References

[1] Saravanan, M., Rahul Deepak, R. S., Ravinkumar, P. L. & Sivabaalavignesh, A. Vehicle communication using visible light (Li-Fi) technology. in *2022 8th International Conference on Advanced Computing and Communication Systems (ICACCS)* 885–889 (2022). https://doi.org/10.1109/ICACCS54159.2022.9785174

[2] Aly, B., Elamassie, M. & Uysal, M. Vehicular VLC system with selection combining. *IEEE Trans. Veh. Technol*. **71**, 12350–12355 (2022). https://doi.org/10.1109/TVT.2022.3192329

[3] Mamatha, K. R & Pavithra, S. Visible light communication in intelligent transportation system for I2V and V2V mode. *Int. Res. J. Eng. Tech*. **5**, 3084–3090 (2018). https://www.irjet.net/archives/V5/i5/IRJET-V5I5590.pdf

[4] Jin, W.-L., Kwan, C., Sun, Z., Yang, H. & Gan, Q. *SPIVC: A Smartphone-Based Inter-Vehicle Communication System*. (University of California, 2012) http://www.its.uci.edu/~wjin/publications/SPIVC.v5.pdf

[5] Azzedine, B., Oliveira, H.A.B.F, Nakamura, E.F. & Loureiro, A.A.F. Vehicular ad hoc networks: a new challenge for localization-based systems. *Comput. Commun*. **31**, 2838–2849 (2018). https://doi.org/10.1016/j.comcom.2007.12.004

[6] Rima, D. & Sanya, A. Performance analysis of DF based mixed VLC-FSO-VLC system. in *International Conference on Signal Processing and Communications (SPCOM)* 1–5 (2020). https://doi.org/10.1109/SPCOM50965.2020.9179534

[7] Haas, H., Yin, L., Wang, Y. & Chen, C. What is LiFi? *J. Light. Technol*. **34**, 1533–1544 (2016). https://doi.org/10.1109/JLT.2015.2510021

[8] Khalighi, M. A. & Uysal, M. Survey on free space optical communication: a communication theory perspective. *IEEE Commun. Surv. Tutor*. **16**, 2231–2258 (2014). https://doi.org/10.1109/COMST.2014.2329501

[9] Ghassemlooy, Z., Popoola, W. & Rajbhandari, S. *Optical Wireless Communications: System and Channel Modelling with Matlab* (CRC Press, 2013).

[10] Niu, M., Cheng, J. & Holzman, J. F. Error rate performance comparison of coherent and subcarrier intensity modulated optical wireless communications. *J. Opt. Commun. Netw*. **5**, 554–564, (2013). https://doi.org/10.1364/JOCN.5.000554

[11] Basnayaka, D. A., & Haas, H. Hybrid RF and VLC systems: Improving user data rate performance of VLC systems. in *IEEE 81st Vehicular Technology Conference (VTC)* 1–5 (2015). https://doi.org/10.1109/VTCSpring.2015.7145863

[12] Kazemi, H., Uysal, M., & Touati, F. Outage Analysis of Hybrid FSO/RF Systems Based on Finite-State Markov Chain Modeling. in *3rd International Workshop in Optical Wireless Communications (IWOW)* 11–15 (2014). https://doi.org/10.1109/IWOW.2014.6950767

[13] Momen, M. M. A., Fayed, H. A., Aly, M. H., Ismail, N. & Mokhtar, A. An efficient hybrid visible light communication/radio frequency system for vehicular applications. *Opt. Quant. Electron*. **51**, 364 (2019). https://doi.org/10.1007/s11082-019-2082-7

[14] Abaza, M., Mesleh, R., Mansour, A. & Aggoune, E. H. M. Relay Selection for Full-Duplex FSO Relays over Turbulent Channels. in *IEEE International Symposium on Signal Processing and Information Technology (ISSPIT)* 103–108, (2016). http://ali.mansour.free.fr/PDF/ISSPIT2016_2.pdf

[15] Farid, A. A. & Hranilovic, S. Outage capacity optimization for free-space optical links with pointing errors. *J. Light. Technol*. **25**, 1702–1710 (2007). https://doi.org/10.1109/JLT.2007.899174

[16] Solomonovich, G. I. & Moiseevich, R. I. *Table of Integrals, Series, and Products*. (Academic Press, 2007).

[17] Elgala, H., Mesleh, R. & Haas, H. Indoor optical wireless communication: potential and state-of-the-art. *IEEE Commun. Mag.* **49**, 56–62, (2011). https://doi.org/10.1109/MCOM.2011.6011734

[18] Taher, M. A., Abaza, M., Fedawy, M. & Aly, M. H. Relay selection schemes for FSO communications over turbulent channels. *Appl. Sci*. **9**, 1281 (2019). https://doi.org/10.3390/app9071281

[19] Abaza, M., Mesleh, R., Mansour, A. & Aggoune, E. M. The performance of space shift keying for free-space optical communications over turbulent channels. *Proc. SPIE* **9387,** 1–8 (2015). https://doi.org/10.1117/12.2076528

[20] Akanegawa, M., Tanaka, Y., & Nakagawa, M. Basic study on traffic information system using LED traffic lights. *IEEE Trans. Intell. Transp. Syst*. **2**, 197–203 (2001). https://doi.org/10.1109/6979.969365

[21] Kahn J. M. & Barry, J. R. Wireless infrared communications. *Proc. IEEE* **85**, 265–298 (1997). https://doi.org/10.1109/5.554222

[22] Cailean, A. M., Cagneau, B., Chassagne, L., Popa, V. & Dimian, M. Evaluation of The Noise Effects on Visible Light Communications Using Manchester and Miller Coding. in *International Conference on Development and Application Systems (DAS)* 85–89 (2014). https://hal.archives-ouvertes.fr/hal-01207160/document